Temperature and thermodynamic instabilities in heavy ion collisions

C. Fuchs [a], P. Essler [b], T. Gaitanos [b], H. H. Wolter [b]

[a]*Institut für Theoretische Physik der Universität Tübingen, D-72076 Tübingen, Germany*

[b]*Sektion Physik, Universität München, D-85748 Garching, Germany*

Abstract

We investigate thermodynamic properties and instability conditions in intermediate energy heavy ion reactions. We define locally thermodynamic variables, i.e. density, pressure and temperature, directly from the phase space distribution of a relativistic transport calculation. In particular, temperatures are determined by a fit to two covariant hot Fermi distributions thus taking into account possible anisotropic momentum configurations. We define instability independent from the nuclear matter spinodal by the criterion that the effective compressibility becomes negative. The method is applied to a semi–central Au on Au reaction at 600 MeV/nucleon. We investigate in particular the center of the participant and the spectator matter. In the latter we find a clear indication of instability with conditions of density and temperature that are consistent with experimental determinations.

Key words: Liquid-gas phase transition, temperature, thermodynamic instabilities, relativistic BUU, Au+Au, E=600 MeV/nucleon reaction.
PACS numbers: **25.75.-q**, 25.60.Gc, 25.70.Mn,

1 Introduction

One of the challenges in the investigation of heavy ion collisions is the understanding of the multi–fragmentation process which is observed in the final stages of such reactions. The mass spectra are observed to follow a power law which leads to the concept of a first–order liquid–gas phase transition or even of second–order critical behavior. Recently a first order phase transition seems to have been found by the ALADIN collaboration [1,2] from spectator fragments in Au + Au collisions at 600 A.MeV, but this interpretation is still under much debate, in particular with respect to the correct thermometers to be used [2].

Equally the theoretical description of the fragmentation process is widely debated. The models can be roughly divided in two classes, dynamical models based on transport equations [3–8] and statistical models based on the assumption of local thermal equilibrium [9,10]. Transport models as BUU, however, are mean field models which describe the evolution of the one–body phase space density under the action of the mean field and the average action of the collision term. For the fragmentation process, however, correlations beyond the mean field are decisive whenever the system enters an instability region. These higher order correlations have been reintroduced as fluctuations in various ways: (1) by adding a fluctuation term, leading to a Boltzmann–Langevin (BL) equation [3–5], (2) by choosing the numerical fluctuation in a judicious way by the number of test particles [6], or (3) by introducing fluctuations directly into the phase space distribution [11]. The detailed consequences of these approaches are presently under intense investigation.

On the other hand, mean field dynamics governs the system as long as it remains in stable regions of phase space. This is the case also after an instability point, when the system has attained a new stable configuration. In fact, within a mean field approach one should be able to determine when the system enters

instability regions, and also the characteristic thermodynamical state of this situation, i.e. its density, pressure, temperature, isotopic ratios etc. It is also clear that these critical values need not be the same in the finite colliding system as in nuclear matter. Nuclear matter instability is a pure volume effect, while in a heavy ion collision finite size effects, in particular surface effects, should be of great importance. Even though in a mean field approach one will not be able to predict how the instable system breaks up, one can therefore still determine the conditions at which this occurs. This is not only an important input for models of statistical breakup or dynamical fluctuations, it can also be compared to experimental determinations of the fragmenting source.

The idea of the present work is then to investigate instability situations within mean field dynamics, i.e. within transport calculations [12]. In doing so we want to take account of the fact that different thermodynamical conditions are expected to prevail in different regions and at different times in the collision process. We therefore determine the thermodynamic variables locally. As a local criterion for instability we use a thermodynamical condition, namely that the quantity $K_{\text{eff}} = 9\frac{\partial P}{\partial \rho}$ becomes negative. We thus define K_{eff} as an effective compressibility for the finite systems which need not be the same as for infinite nuclear matter or for the ground state of nuclei. Other criteria that have been used are the growth of numerical fluctuations [6] or a positive Lyapunov exponent [7]. We believe that the present criterion defines a dynamical instability.

A particular difficulty is the determination of a temperature, and different approaches have been used for this. It is clear that at energies above about 100 A.MeV the system is globally not in equilibrium and therefore a temperature determined from the global momentum distribution is not reasonable [13]. However, even the local momentum distribution need not to be equilibrated, in fact, as will be seen later, the two subsystems are still well separated in momentum space through much of the process. In this situation the momentum

3

distribution may still be represented as that of two equilibrated subsystems of finite temperature [14] and we also follow this approach here. It is still a question of debate, how such temperatures should be compared to the various experimental thermometers, as e.g. slope parameters of particle spectra [15], excited state or isotopic ratios [1]. Certainly slope parameters correspond least well to the temperatures determined here.

As a realization of transport equations we use the relativistic Landau–Vlasov (RLV) method, which was originally introduced in Ref. [16] and relativistically extended in Ref. [17]. It uses covariant Gaussian test particles in coordinate and momentum space and thus allows to calculate truly local quantities at every space–time point. It is thus particularly suited for the present purpose.

We apply the investigation to Au on Au collisions at 600 A.MeV energy which has been extensively investigated by the ALADIN [1,2] and FOPI [18] collaborations in particular with respect to possible phase transitions. We have previously investigated this reaction at 400 MeV in Ref. [19] in particular with respect to the interactions to be used, the question of non–equilibrium effects, and the determination of the equation–of–state. Since here our main emphasis is on the investigation of instability conditions, we use a simpler standard interaction. We study a semi–central collision, where we can distinguish clearly a central participant and a spectator region, which should behave very differently with respect to their thermodynamical evolution.

2   Determination of local thermodynamic properties

In equilibrated nuclear matter the pressure P is isotropic and the energy-momentum tensor $T^{\mu\nu}$ takes the same form as in an ideal fluid [20]

$$T^{\mu\nu}(x) = [\epsilon(x) - P(x)]\, u^{\mu}(x) u^{\nu}(x) - P(x) g^{\mu\nu} \quad . \tag{1}$$

4

The streaming velocity $u_\mu = j_\mu/\rho_0$ is obtained from the baryonic current

$$j_\mu(x) = 4 \int \frac{\mathrm{d}^4 k}{(2\pi)^3} k_\mu^* f(x, k) \qquad (2)$$

where the phase space distribution f is related to the local momentum distribution n as

$$f(x, k) = n(x, \vec{k}) \delta \left(k^{*2} - m^{*2} \right) 2\Theta(k_0^*) \quad . \qquad (3)$$

The Lorentz invariant baryon rest density is defined as

$$\rho_0 = \sqrt{j_\mu j^\mu} = \rho_\mathrm{B}|_\mathrm{restframe} \quad . \qquad (4)$$

In the rest frame of equilibrated nuclear matter the momentum distribution is given by a diffuse Fermi sphere or, in a general frame, by a diffuse Fermi ellipsoid

$$n(x, \vec{k}, T) = \frac{1}{1 + \exp\left[-(\mu^* - k_\mu^* u^\mu)/T \right]} \qquad (5)$$

with the temperature T, the effective chemical potential $\mu^*(T)$ and $k_0^* = E^* = \sqrt{\vec{k}^{*2} + m^{*2}}$. In the case of vanishing temperature Eq. (5) reduces to a sharp Fermi ellipsoid

$$\lim_{T \to 0} n(x, \vec{k}, T) = \Theta \left(E_\mathrm{F} - k_\mu^* u^\mu \right) \qquad (6)$$

with the chemical potential given by the Fermi energy $E_\mathrm{F} = \sqrt{m^{*2} + k_\mathrm{F}^2}$.

In these expressions the effective mass $m^* = M - g_\sigma \Phi(x)$ and the kinetic four-momenta $k_\mu^* = k_\mu - g_\omega \omega_\mu(x) - \frac{e}{2}(1 + \tau_3)A_\mu(x)$ are shifted by the scalar Φ and vector meson ω_μ fields, respectively and a Coulomb four-vector potential A_μ is added and treated in a action-at-a-distance formulation [21].

By definition Eq.(1) already contains the case of a collective motion of the matter as a whole, e.g., in a radially expanding source $u_\mu = (\gamma, \gamma\vec{\beta})$ is given by a radial flow $\vec{\beta}$ and only vanishes in the local rest frame. However, in the time evolution of a heavy ion collision the situation of equilibrated nuclear matter, Eq.(1), is the exception. Through most of the reaction the system is *not* in local equilibrium. Except for special cases as, e.g., in the final fireball or in the spectator matter, the pressure is not isotropic but rather has to be decomposed into contributions transversal and longitudinal to the relative velocity of the currents. We choose the z–axis as the beam direction. Then the pressure components follow from the energy momentum tensor ($i = 1, 2, 3$ correspond to x, y, z) as

$$P_\perp = \frac{1}{2}\left(T^{11} + T^{22}\right) \quad , \quad P_\parallel = T^{33} \quad . \tag{7}$$

$P_\perp$ and $P_\parallel$ are determined in the local rest frame which in colliding nuclear matter is the center-of-mass frame of the two currents where the total baryon current vanishes [22]. Thus, the difference of $P_\perp$ and $P_\parallel$ also yields a measure for the equilibration of the system.

Although the total system is not in local equilibrium the single currents of their own may be so. In actual calculations it is found, that the phase space can be well approximated by configurations close to the initial one, i.e. by two separated Fermi spheres [14] or, covariantly, by two separated Fermi ellipsoids, which correspond to colliding nuclear matter currents [19]. We therefore approximate the phase space by colliding nuclear matter configurations as described in Refs. [19,22], however, in the present work of non-zero temperature. These configurations are represented as [23]

$$n^{(12)} = n^{(1)} + n^{(2)} - \delta n^{(12)} \quad , \tag{8}$$

where $\delta n^{(12)} = \sqrt{n^{(1)} \cdot n^{(2)}}$ is a Pauli correction which guarantees the validity of the Pauli principle in the case that the currents $n^{(1)}$ and $n^{(2)}$ overlap. The single distributions $n^{(i)}$ are given by Eq.(5). In principle the temperatures T_1 and T_2 can be different. The collective parameters $u_{1\mu}$, $u_{2\mu}$, and $\mu_1^*(T_1)$, $\mu_2^*(T_2)$ are determined from the phase space distribution by a decomposition into contributions stemming from projectile and target $f(x, k) = f^{(1)}(x, k) + f^{(2)}(x, k)$ [19]. In the limit of a vanishing relative velocity the ansatz of eq. (8) provides a smooth transition from the non-equilibrium colliding nuclear matter configuration to the equilibrated one, i.e. $n^{(12)} \longmapsto n$. Furthermore the asymptotic state of two cold $(T = 0)$ currents is naturally included in this description.

The local temperature is obtained from a least square fit of the expression given by Eqs. (5) and (8) to the momentum distribution $n(x, \vec{k})$, Eq. (10), obtained from the relativistic transport calculation [17]. In this fit only the temperatures are treated as free parameters. The streaming velocities are determined directly from the respective currents, Eq. (2), and the chemical potentials $\mu_i^*(T_i)$ entering into Eq. (8) are obtained by the requirement of total baryon number conservation

$$j_0(x) = 4 \int \frac{\mathrm{d}^3 k}{(2\pi)^3} n^{(12)}(x, \vec{k}, T) \tag{9}$$

by iteration.

As discussed in the introduction we use as a realization of the transport equation the relativistic Landau–Vlasov (RLV) method, which makes use of covariant Gaussian test particles in coordinate and momentum space [17]. The RLV momentum space distribution is given by

$$n(x, \vec{k}) = \frac{(2\pi)^3}{4} \frac{1}{N(\pi\sigma\sigma_{\mathrm{k}})^3} \sum_{i=1}^{A \cdot N} \mathrm{e}^{[(x_\mu - x_{i\mu})^2 - ((x_\mu - x_{i\mu})u_i^\mu)^2]/\sigma^2} \, \mathrm{e}^{(k^{*2} - (k_\mu^* u_i^\mu)^2)/\sigma_{\mathrm{k}}^2} \tag{10}$$

and in our particular calculations we use $N = 100$ testparticles per nucleon and $\sigma = 1.40$ fm, $\sigma_{\mathrm{k}} = 0.346$ fm^{-1} as the width of the Gaussian in co-

ordinate and momentum space, respectively. This allows us to calculate all quantities locally without recourse to discretization in cells. There is, however, a technical point to be noted. The finite width of the momentum space gaussians leads to a smearing of the local momentum distribution $f(x, k)$, which would be interpreted as an artificial temperature, when fitted with the expression of Eqs. (5) or (8). Thus even for a initialized cold nucleus finite temperatures are obtained depending on σ_{k}, the width of the gaussians in momentum space (in our case about $T \sim 5$ MeV). To take this into account the configurations, Eqs. (5) and (8), are first folded over the momentum space gaussian. The folding procedure is defined covariantly as $\tilde{n}(x, \vec{k}, T) = \int \mathrm{d}^4 k' m^* n(x, \vec{k}', T) g(k' - k) \delta(k^{*\prime 2} - m^{*2}) 2\Theta(k_0^{*\prime})$. The momentum space gaussian $g(k')$ is defined as in (10), however, with the streaming velocity of the current, Eq. (2), instead of the particle velocity. The folding is most naturally performed in the rest frame of the current where the expression reduces to a folding over a standard gaussian, i.e.

$$\tilde{n}(x, \vec{k}, T) = \int \frac{\mathrm{d}y^3 k'}{\sqrt{\pi \sigma_{\mathrm{k}}^2}^3} \frac{m^*}{E^{*\prime}} n(x, \vec{k}', T) \, \mathrm{e}^{-(\vec{k}^{*\prime} - \vec{k}^*)^2 / \sigma_{\mathrm{k}}^2} \qquad .$$

In the case of colliding nuclear matter configurations (8) this procedure has to be performed separately for each current. Thus artificial temperature effects are eliminated and reliable initial values are obtained ($T \sim 0.5$ MeV) which are a very good starting point for the numerical analysis.

3   Thermodynamic properties of Au on Au at 600 A.MeV

The analysis described above is applied to a typical intermediate energy reaction, i.e. a semi-central (b=4.5 fm) Au on Au reaction at 600 A.MeV. This same reaction was also investigated in Ref. [19] at 400 A.MeV with the RLV method [17]. It has been extensively studied by the FOPI and ALADIN col-

laboratories at GSI [1,2,18]. In relativistic models the mean field originates from the cancelation of large scalar and vector fields. Realistic mean fields derived from the Dirac-Brueckner G-matrix and which also account for non-equilibrium aspect of the phase space [22] were, e.g. used in the calculations in Ref. [19]. However, for simplicity, in the present work we use the standard parameterization of the non-linear Walecka model (NL2) [13], which was also used for comparison in Ref. [19].

In Fig. 1 we demonstrate the basic idea of the present approach. The left hand column gives density contours at different times of the collision (10,50,60 fm/c). The two columns to the right give contours of local momentum distributions, the one obtained in the RLV calculation in the middle and the one fitted according to eq. (8) to the right with the fit values of the temperature also given. The two upper rows show the momentum distribution in the center, the lower one in the spectator moving to the left.

It is seen that after 10 fm/c the temperature is already high in the center (T=34.6 MeV), however, the ellipsoids corresponding to projectile and target are still well separated. Thus the configuration is highly anisotropic and is well represented by two hot and counterstreaming currents of nuclear matter. At 50 fm/c the system has reached local equilibrium in the center and has also strongly cooled down (T=5.4 MeV). Thus we find that as long as temperatures are high non-equilibrium aspects of the phase space are of major importance. At the later stages where equilibrium is reached the system cannot really be considered as a " fireball " since the temperature is already low. However, in both cases the phase space is well approximated by the parameterization of eq. (8) which describes one or two equilibrated subsystems. The spectator is clearly identified in the density contour plots at the later stages. In the spectator the momentum space is well represented by one Fermi fluid and the temperature is well defined and found to be low.

We next look at the evolution of density and temperature in the central and spectator regions. We will put more emphasis on the discussion of the spectator since it will be seen to be the more interesting part. In the following analysis we identify the spectator region at each time step from inspection of the evolution of the density profile and extract the respective observables at the position of maximum density.

In Fig. 2 the evolution of the density is shown for the spectator and in the center (insert). In the center we see the typical compression–decompression behavior. The total density rises to about 2.5 ρ_{sat} and then continuously falls to zero. The spectator density decreases in the decompression phase from about saturation density ($\rho_{\mathrm{sat}} = 0.145$ fm^{-3} in the present model) to a value of $\sim \frac{1}{3}\rho_{\mathrm{sat}}$ where it then stays relatively constant over a period of 30 fm/c before the spectator completely evaporates.

In Fig. 3 we show the corresponding evolution of the local temperature again for spectator and central (insert) regions. For the temperature in the central " fireball " region we obtain a maximum value of about 40 MeV and a mean temperature of about 30 MeV over the duration of the compression phase. Thus the present phase space analysis results in significantly smaller temperatures than those extracted from particle spectra [15]. This indicates that temperatures determined from the slope parameters of such spectra apparently overestimate the real temperature by at least a factor of two. Similar results have been found in Ref. [24]. However, the present results are in qualitative agreement with temperatures extracted experimentally from a flow analysis within the blast scenario. E.g., in Ref. [18] a value of $T = 36.7 \pm 7.5$ MeV has been found in Au on Au collisions at 400 A.MeV.

The temperature in the spectator shows a rather different behavior. When the spectator region is clearly developed in the transport calculation its temperature is about 15 MeV and then continuously decreases to a value around 5

MeV where it stays fairly stable. Thus density and temperature in the spectator both show a sort of plateau between about 50 and 85 fm/c. It is seen later that this phase seems to correspond to a region of instability.

To study this further we now investigate $P - \rho_0$ diagrams, which show the thermodynamical evolution of the system as a trajectory with time as a parameter. Since we have defined $K_{\text{eff}} = 9\frac{\partial P}{\partial \rho_0}$ as the effective compressibility a negative slope of this trajectory signifies that the system enters a region of instability. At this point the system is expected to be sensitive to fluctuations and eventually to form fragments.

In Fig. 4 we show the evolution of the central region in the $P - \rho_0$ diagram. In the following ρ_0 corresponds to the local rest density, Eq. (4) and thus a distortion of the results by Lorentz effects is eliminated. It can be seen that the pressure is mostly positive and is maximal in a very early stage of the reaction ($t = 10 - 15$ fm/c) and then rapidly drops down to values around zero ($t \sim 10 - 15$ fm/c). In the compression phase which lasts from about 10–30 fm/c (see also Fig. 2) the pressure is highly anisotropic, i.e. the longitudinal component is more than twice as large as the transversal one. After 30 fm/c both components have approached values close to zero. The respective maximum values $P_{\parallel} = 80$ MeV fm^{-3}, $P_{\perp} = 30$ MeV fm^{-3} are in qualitative agreement with the analysis of Ref. [13] where, however, only global quantities have been considered. A thermodynamic instability region, i.e. a negative slope of the $P - \rho_0$ trajectory, occurs after 60 fm/c. This is not seen within the scale of the figure, because the density is already very low (Fig. 2). Therefore one does not expect the formation of larger fragments in the central region.

In Fig. 5 we show the corresponding $P - \rho_0$ diagram for the spectator matter. The pressure is now negative for densities below saturation which reflects the van-der-Waals like behavior of the nuclear matter equation of state also in

the finite system. Furthermore, the spectator is not completely equilibrated even at the later stages of the reaction since longitudinal and transversal components are still significantly different in magnitude. They show, however, a very similar behavior in their phase trajectories. It is seen that after 45 to 50 fm/c both the longitudinal and the transverse pressures increase with decreasing density and thus the compressibility becomes negative. As discussed in connection with Fig. 3 the temperature is rather stable after this point. This ensures that a thermodynamic compressibility $K_{\mathrm{eff}} = 9\frac{\partial P}{\partial \rho_0}|_{T=\mathrm{const}}$ can be defined in a meaningful way, i.e. the change of the local pressure occurs in good approximation at constant temperature. The system at this stage therefore enters an instability region and should break up into fragments. The break up density lies between $(\frac{1}{3} - \frac{1}{2})\rho_{\mathrm{sat}}$. In the present analysis the value of $T = 5$ MeV corresponds to the break up temperature. Thus it is in rather good agreement with the experimental value of the critical temperature at the liquid-gas phase transition measured by the ALADIN Collaboration for the same reaction [1].

As discussed, a description of the break up process is beyond the scope of a mean field approach. In the mean field calculation the system remains in a relatively stable configuration at densities around $\frac{1}{3}\rho_{\mathrm{sat}}$ which lasts over a period from 60 to 85 fm/c before the spectator completely evaporates.

In fig. 5 we have underlaid the isothermal equation–of–state for thermalized nuclear matter for temperatures of 5 and 9 MeV, which correspond to the range of temperatures determined for the spectator (see Fig. 3). The nuclear matter spinodal region is that part of the curves, where the slope is negative. As stressed before the instability conditions, as determined here, do not have to be identical to those of nuclear matter. However, it is seen that in the final stages of its evolution (after about 65 mf/c) the spectator rather closely follows the nuclear matter behavior, as one would perhaps expect. Before that, the thermodynamic conditions are appreciably different from those of

thermalized nuclear matter. In the early stages of the spectator ($t < 40$ fm/c) the pressures are higher because there is not yet a clear separation of spectator and participant. While the critical density, where instability sets in, is about the same the pressures are different and there is still substantial anisotropy. Therefore it is to be expected that the fragmentation process which is initiated by fluctuations at this point is strongly influenced by these conditions. Thus for the treatment of multi–fragmentation the treatment of these dynamical instabilities is very important.

4 Conclusions

The purpose of the present work is to investigate in the framework of transport theories the thermodynamical state of matter in a heavy ion collision, in particular with respect to the occurrence of instabilities. It is argued that this can be answered in a mean field treatment, while the further evolution and possible fragmentation depends on fluctuations and is beyond this approach. To this end we determine thermodynamic variables directly from the local momentum distribution. In particular, temperature is obtained by a fit to two hot Fermi distributions, respecting the Pauli principle, thus taking into account the most typical non–equilibrium effect in a heavy ion collision. In this way the three intensive variables T, P, ρ are determined independently from each other, while in a specific system, e.g. in nuclear matter, they are, of course, constrained by the equation–of–state. A comparison therefore shows the effect of finite size and non–equilibrium effects on the thermodynamical state. As a criterion for instability we use a negative effective compressibility defined from the local thermodynamic variables. Thus we use the concept of a dynamical instability which is different, in principle, from the static spinodal instability in nuclear matter.

We applied these methods to the typical, semi-central, well–studied, inter-

mediate energy reaction Au+Au at 600 A.MeV and investigate the central and the spectator zones. We determine thermodynamical variables which are largely consistent with experimental determinations. In particular we see an instability develop in the heated spectator, which should then lead to spectator multi–fragmentation as observed in the ALADIN collaboration. Also the breakup temperatures and densities are in reasonable agreement. We see that the thermodynamical variables thus determined are different from the nuclear matter equation–of–state. The determination of instability situations is important for the description of multi–fragmentation in other theories: for the application of statistical approaches one has to know whether the breakup configuration is equilibrated and what are its parameters; for dynamical treatments of fluctuations, as in the various approaches to the BL–equation, it is important to know, at what points in the evolution fluctuations are important and what is their magnitude. The present analysis will be extended in the future to a more systematic study of heavy ion collisions, in particular also to less symmetric points. This will allow to also study collective flow and temperature in the context of radial flow scenarios.

References

[1] J. Pochodzalla and the ALADIN Collaboration, Phys. Rev. Lett. 75 (1995) 1040.

[2] W. Trautmann and the ALADIN Collaboration, Proc. of the 35th International Winter Meeting on Nuclaer Physics, Bormio, Italy, 1997, ed. by I. Iori.

[3] S. Ayik, C. Gregoire, Nucl. Phys. A 513 (1990) 187.

[4] J. Randrup and B. Remaud, Nucl. Phys. A 514 (1990) 339.

[5] Y. Abe, S. Ayik, P. G. Reinhard, E. Suraud, Phys. Rep. 275 (1996) 49.

[6] M. Colonna, M. Di Toro, A. Guarnera, V. Latora and A. Smerzi, Phys. Lett. B 307 (1993) 273;
M. Colonna, M. Di Toro, A. Guarnera, Nucl. Phys. A 589 (1995) 160.

[7] A. Bonasera, V. Latora, A. Rapisarda, Phys. Rev. Lett. 75 (1995) 3434;
M. Belkacem et al., Phys. Rev. C 54 (1996) 2435.

[8] R.K. Puri, Ch. Hartnack, J. Aichelin, Phys. Rev. C (1995) R28.

[9] J.P. Bondorf, R. Donangelo, I.N. Mishustin, C.J. Pethik, H. Schulz and K. Sneppen, Nucl. Phys. A 443 (1985) 321.

[10] D.H.E. Gross, X. Z. Zhang and S. Y. Xu, Rev. Lett. 56 (1986) 1544;
A. S. Botvina, D.H.E. Gross, Nucl. Phys. A 592 (1995) 257.

[11] M. Colonna, M. di Toro, S. Maccarone, M. Zielniska–Phabe, A. Guarnera, Proc. of CRIS '96, Acicsstello, Italy, ed. S. Costa et al., World Scientific 1996.

[12] P. Essler, H. H. Wolter, C. Fuchs, Proc. of CRIS '96, Acicsstello, Italy, ed. S. Costa et al., World Scientific 1996.

[13] A. Lang, B. Blättel, W. Cassing, V. Koch, U. Mosel and K. Weber, Z. Phys. A 340 (1991) 287.

[14] R.K. Puri, N. Ohtsuka, E. Lehmann, A. Faessler, M.A. Matin, D.T. Khoa, G. Batko, S.W. Huang, Nucl. Phys. A 575 (1995) 733.

[15] L. Venema and the TAPS Collaboration, Phys. Rev. Lett. 71 (1993) 835;
O. Schwalb and the TAPS Collaboration, Phys. Lett. B 321 (1994) 20;
C. Müntz and the KaoS Collaboration, Z. Phys. A 352 (1995) 175.

[16] C. Gregoire, B. Remaud, F. Sebille, L. Vincet, and Y. Raffay, Nucl. Phys. A 465 (1987) 317.

[17] C. Fuchs, H.H. Wolter, Nucl. Phys. A 589 (1995) 732.

[18] W. Reisdorf and the FOPI Collaboration, Nucl. Phys. A 612 (1997) 493.

[19] C. Fuchs, T. Gaitanos, H.H. Wolter, Phys. Lett. B 381 (1996) 23.

[20] S.R. de Groot, W.A. van Leeuwen, C.G. van Weert, *Relativistic Kinetic Theory*, (North Holland, Amsterdam, 1980).

[21] H. Feldmeier, M. Schönhofen, M. Cubero, Nucl. Phys. A 495 (1989) 337c.

[22] L. Sehn, H.H. Wolter, Nucl. Phys. A 601 (1996) 473;
C. Fuchs, L. Sehn, H.H. Wolter, Nucl. Phys. A 601 (1996) 505.

[23] L. Sehn, thesis, München, 1991 (unpublished).

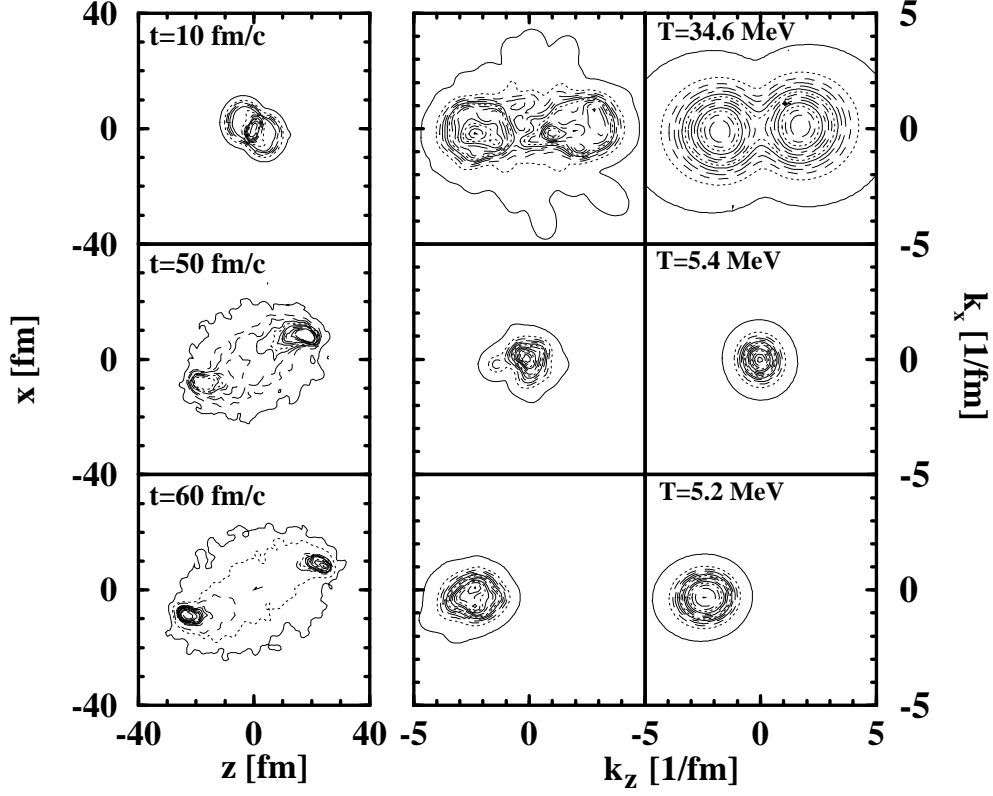[24] J. Konopka, H. Stöcker and W. Greiner, Nucl. Phys. A 583 (1995) 357.

Fig. 1. Phase space distributions in the semi–central (b = 4.5 fm) Au+Au reaction at 600 A.MeV. The three rows correspond to times t = 10, 50, and 60 fm/c. The left-most column gives the density contours, the two right hand ones local momentum distributions as obtained from the transport calculations (middle) and by a fit with one or two hot Fermi–ellipsoids (right) with temperatures indicated. In the first two rows the momentum distributions are shown for the center, in the last row for the spectator.
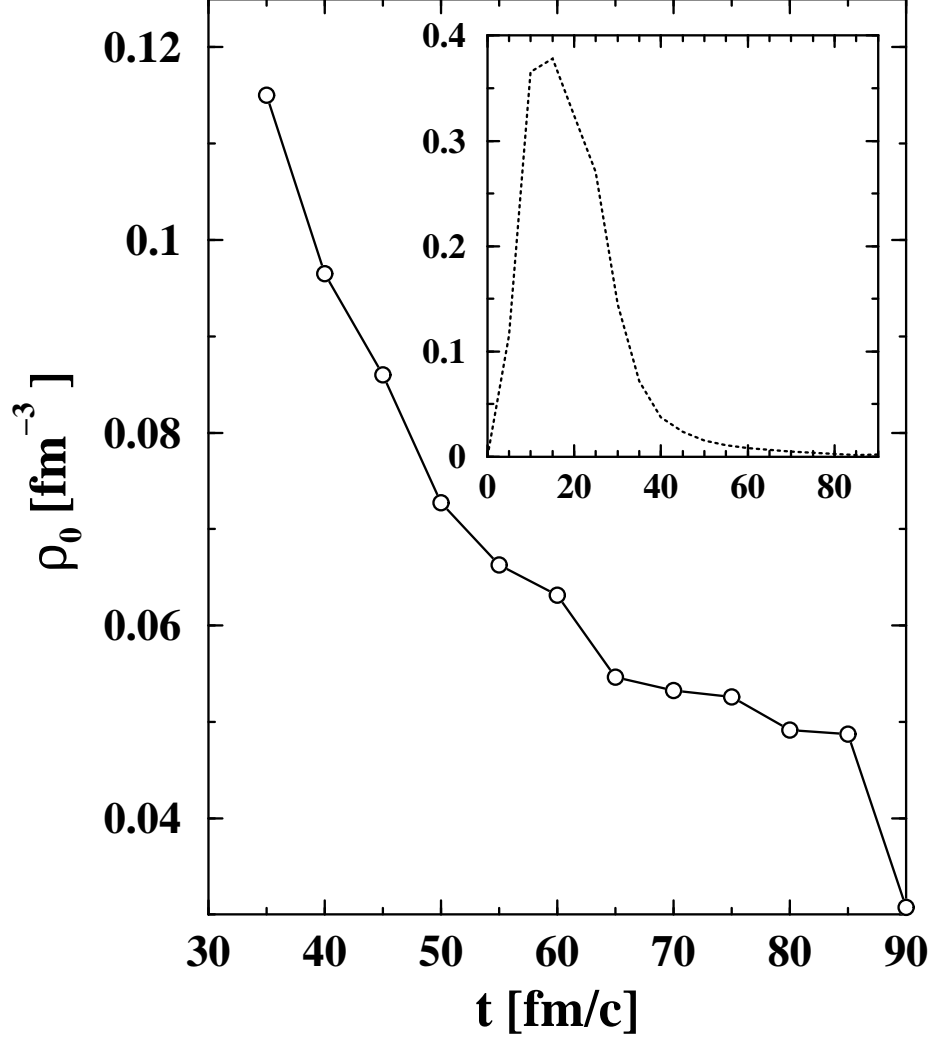
Fig. 2. Time evolution of the local total density in the spectator matter in a semi-central Au on Au rection at 600 A.MeV. The insert shows the corresponding density in the center.
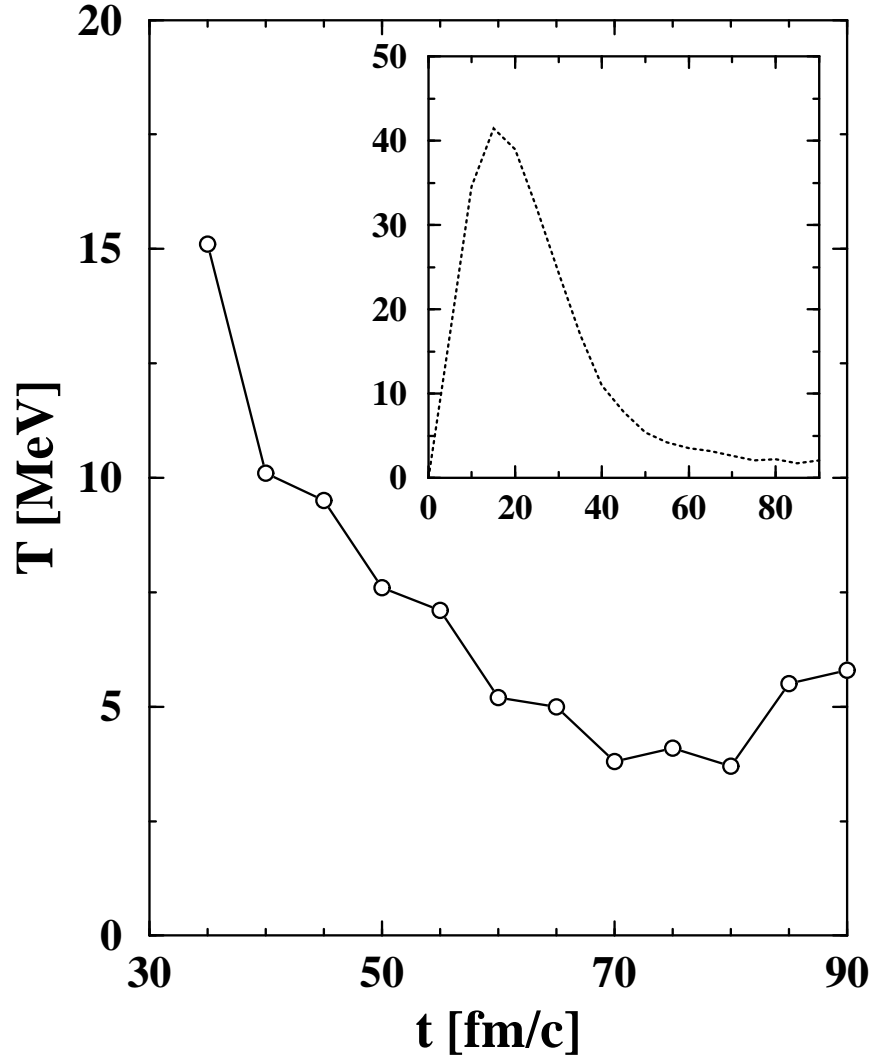
Fig. 3. Time evolution of the local temperature of the spectator matter in a semi-central Au on Au rection at 600 A.MeV. The insert shows the corresponding temperature obtained in the center.
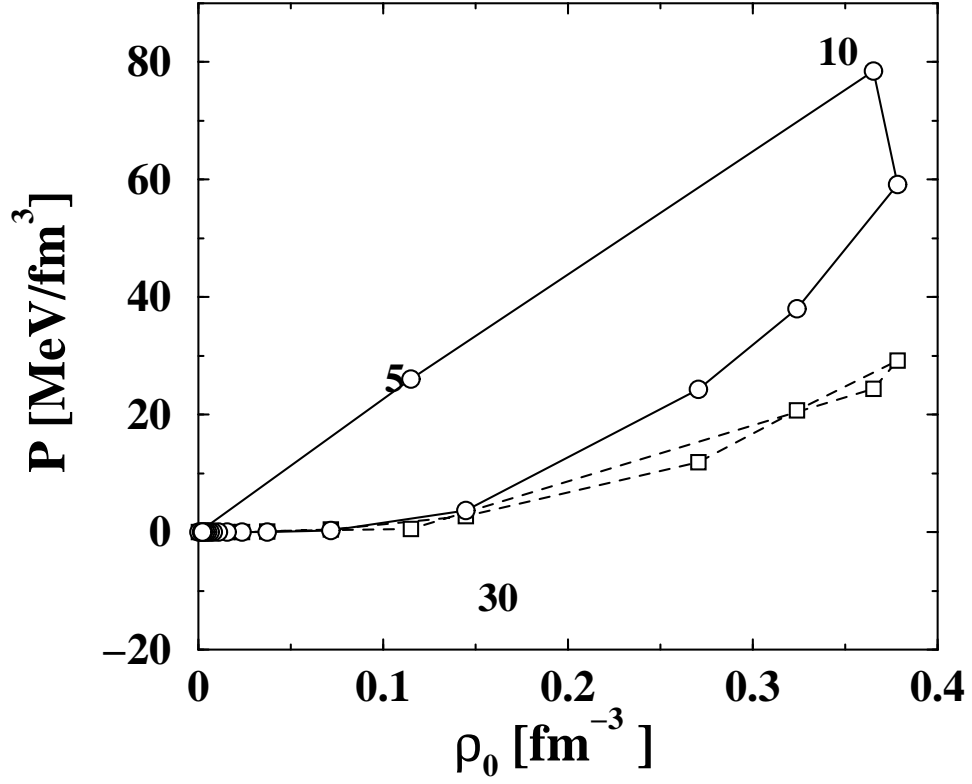
Fig. 4. Density-pressure trajectory in the center obtained in a semi-central Au on Au reaction at 600 A.MeV. The evolution of longitudinal (solid line) and transverse (dashed line) pressure is shown separately. The corresponding times (fm/c) are indicated for some cases points (the difference between points is 5 fm/c).
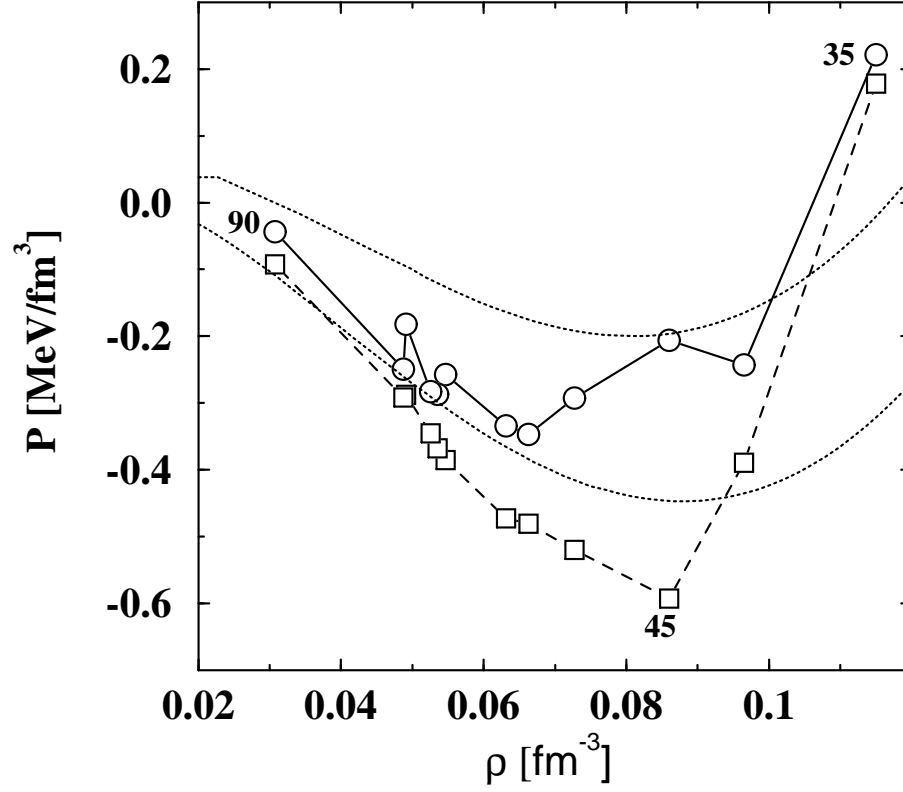
Fig. 5. Density-pressure trajectory for the spectator matter in a semi-central Au on Au reaction at 600 A.MeV as in Fig. 4. The dotted curves are the nuclear matter equation of state for T = 5 and 9 MeV (lower and upper curve, respectively).